Decreasing Carrier Mobility under Concentrated Illumination and Its Effect on the Series Resistance and Conversion Efficiency of Silicon Concentrator Solar Cells

Tomoki Harada,* Kyosuke Yamashita, Tetsuo Ikari, and Atsuhiko Fukuyama

The carrier mobility of solar cell materials is a critical physical parameter that determines the series resistance. Furthermore, series resistance is an essential factor affecting the conversion efficiency of concentrator solar cells under high sunlight illumination. However, there has been slight discussion regarding the relationship between these factors. In the previous study, it was reported that concentrated illumination decreased carrier mobility; however, the scattering mechanism has not yet been clarified. Moreover, carrier–carrier scattering was discussed; however, it did not cause a mobility reduction. Thus effective mass changes are discussed as a possible cause of the decrease in carrier mobility under concentrated illumination. The cause of the decrease in mobility under concentrated sunlight illumination cannot be fully elucidated; however, it is a change in lattice scattering. Furthermore, the effect of the decrease in mobility due to concentrated illumination on the series resistance and conversion efficiency of Si solar cells using numerical calculations is clarified. The increase in the series resistance caused by the mobility reduction is $\approx$10% under 30 suns.

1. Introduction

Concentrator solar cells have attracted significant attention owing to their low cost and high conversion efficiencies.[1–5] In recent years, concentrator Si tandem solar cells, such as III–V/Si and perovskite/Si solar cells, have been considered for use in automotive solar cells.[6–9] Solar cells with a conversion efficiency of 30% or higher can be operated in most Japanese cars without fossil fuel consumption.[8] The conversion efficiency of concentrator solar cells increases with the logarithm of sunlight concentration (SC).[10] However, the power loss due to series resistance (R_s) reduces the conversion efficiency.[11] A lower R_s is essential for achieving high conversion efficiency.[11,12] R_s is determined by the resistance in the semiconductor layers, contact resistance at the semiconductor–metal interface, and resistance in the metal gridlines. Although several studies have been conducted to reduce R_s, for example, by improving the electrode

geometry,[11,13] there has been little discussion on carrier mobility, which predominantly determines the resistance of the semiconductor layers.

Focusing on the resistance of the semiconductor layers, carrier mobility is essential because it is directly related to the resistivity of the cell material and affects the R_s of solar cells. The decrease in mobility increases the resistivity of the semiconductor material and degrades the carrier transport near the pn-junction, thus degrading the solar cell performance. A discussion on the relationship between mobility and R_s is beneficial for the realization of high-efficiency concentrator solar cells.

We previously discussed the effect of sunlight illumination intensity on mobility using Hall measurements under concentrated sunlight illumination at 300 K.[14] The mobility decreased as the SC increased. We concluded that lattice scattering did not decrease the mobility because the temperature was precisely controlled and fixed during the measurement. Although the scattering processes caused by sunlight illumination have been discussed, we did not find a conclusive origin of the scattering process.[14] Elucidating the reduced mobility under concentrated sunlight illumination will contribute to the development of highly efficient solar cells. Moreover, we did not quantitatively discuss solar cell properties, such as conversion efficiency, short-circuit current (I_{sc}), open-circuit voltage (V_{oc}), and R_s.[14] A quantitative evaluation of the reduced mobility of the solar cells is also necessary. Decreased mobility can reduce the output current and conversion efficiency of solar cells. However, only a few studies, except for those in refs. [14,15], discuss the effects of mobility on the conversion efficiency of concentrator solar cells.

Knowledge of the mobility and R_s of Si under concentrated sunlight illumination is important because, as mentioned earlier, III–V/Si and perovskite/Si solar cells are used as concentrator solar cells for automotive applications. In addition, it can provide insights into improving the performance of concentrator solar cell materials that are not limited to Si. In this study, we discuss the SC- and temperature-dependent mobility of Si to clarify the scattering process under concentrated illumination. The physical properties of Si are well known and well documented, enabling a discussion of the causes of mobility reduction. In addition, the solar cell properties of Si were calculated and discussed by assuming that the decrease in mobility was due to sunlight

T. Harada, K. Yamashita, T. Ikari, A. Fukuyama
Faculty of Engineering
University of Miyazaki
Miyazaki 889-2192, Japan
E-mail: harada.tomoki.q5@cc.miyazaki-u.ac.jp

The ORCID identification number(s) for the author(s) of this article can be found under https://doi.org/10.1002/pssa.202400473.

illumination. Note that this study focuses on electrons because holes can be discussed in a similar manner.

2. Experimental Section

2.1. Hall Measurement under Sunlight Illumination

The Hall measurements were performed using the van der Pauw method.[16,17] Four Ohmic contact electrodes were placed at the corners of the sample. The electrodes were made of aluminum. The n- and p-type Czochralski-grown Si were prepared for the sample, and their carrier concentration in the dark was 4.7 and $5.6 \times 10^{15}\,\mathrm{cm}^{-3}$, respectively. A solar simulator with a 300 W xenon lamp was used as the light source. Standard sunlight (JIS class AAA, 350–1100 nm) was provided using a built-in AM1.5G filter. The SC was varied from 1 to 16 suns (1 sun is $100\,\mathrm{mW\,cm}^{-2}$). Concentrated sunlight was illuminated through an optical fiber and a focusing lens. The temperature was precisely controlled within 0.05 K of the setting temperature using a closed-cycle refrigerator. In addition, a 15 min interval was set between measurements to avoid heat accumulation. Therefore, the temperature increase due to the increase in the SC was negligible in this study. The temperature dependence of the mobility was obtained from 200 to 300 K. Ohmic properties were obtained both in the dark (0 sun) and under 1–16 suns in the temperature range of 200–300 K for both p- and n-type samples.

Electron and hole mobilities were obtained from the measured resistivity and Hall coefficients. Because the carrier concentrations in the dark of the prepared n- and p-type Si were almost equal, the electron and hole mobilities of n- and p-type Si were considered to be the same, even when the carriers were in the majority or minority. The electron and hole mobilities were obtained by substituting the observed resistivity and Hall coefficient into the two-carrier (electron and hole) transport equations, considering the increase in carrier concentration owing to concentrated illumination. Details of the experimental and analytical methods are reported in ref. [14].

2.2. Calculation of Mobility and Solar Cell Properties

2.2.1. Mobility Owing to Carrier Scattering

Lattice and ionized impurity scattering were the dominant scattering processes in the dark.[18–20] Neutral impurity scattering could be ignored because it became important when the concentration was above $10^{18}\,\mathrm{cm}^{-3}$.[21] Another considerable scattering process under sunlight illumination is carrier–carrier scattering. The increased number of photoexcited carriers scatters each other, thus decreasing the mobility.

The electron mobility due to lattice and ionized impurity (μ_L and μ_I) was quoted based on the Arora model.[18,19]

$$\mu_\mathrm{L} = A \times T^{B}\ [\mathrm{cm}^2\,(V \cdot s)^{-1}] \tag{1}$$

$$\mu_\mathrm{I} = \frac{7.3 \times 10^{17} T^{3/2}}{N_\mathrm{I} G(b)}\ [\mathrm{cm}^2\,(V \cdot s)^{-1}] \tag{2}$$

where T represents the temperature in Kelvin, A and B denote the fitting parameters, and N_I denotes the number of

ionized impurity atoms in cm^{-3}. $G(b)$ represents a function expressed as

$$G(b) = \ln(b + 1) - \frac{b}{b + 1} \tag{3}$$

where

$$b = \frac{24 L_\mathrm{D}^2 m_\mathrm{e} k_\mathrm{B} T}{\hbar^2} \tag{4}$$

and

$$L_\mathrm{D} = \sqrt{\frac{\kappa k_\mathrm{B} T}{n q^2}} = \sqrt{\frac{\kappa k_\mathrm{B} T}{(\Delta n + N_\mathrm{I}) q^2}} \tag{5}$$

In these equations, L_D represents the Debye length, $\hbar$ the Dirac constant, m_e the electron conductivity-effective mass, k_B the Boltzmann constant, κ the dielectric constant, q the elementary charge, n the electron concentration in cm^{-3}, and Δn the photoexcited electron concentration in cm^{-3}. The mobility of carrier–carrier scattering (μ_cc) was quoted following the Fletcher model, based on the behavior of gases with positive or negative charges.[21,22]

$$\mu_\mathrm{cc} = 3\pi^{-\frac{1}{2}} 2^{-\frac{3}{2}} (pn)^{-\frac{1}{2}} \kappa^2 q^{-3} \left(\frac{m_\mathrm{e} + m_\mathrm{h}}{m_\mathrm{e} m_\mathrm{h}}\right)^{\frac{1}{2}} (k_\mathrm{B} T)^{\frac{3}{2}}$$
$$\left[\ln\left(1 + 16\kappa^2 (pn)^{-\frac{1}{3}} q^{-4} k_\mathrm{B}^2 T^2\right)\right]^{-1}$$
$$= 3\pi^{-\frac{1}{2}} 2^{-\frac{3}{2}} (\Delta n(\Delta n + N_\mathrm{I}))^{-\frac{1}{2}} \kappa^2 q^{-3} \left(\frac{m_\mathrm{e} + m_\mathrm{h}}{m_\mathrm{e} m_\mathrm{h}}\right)^{\frac{1}{2}}$$
$$\times (k_\mathrm{B} T)^{\frac{3}{2}} \left[\ln\left(1 + 16\kappa^2 (\Delta n(\Delta n + N_\mathrm{I}))^{-\frac{1}{3}} q^{-4} k_\mathrm{B}^2 T^2\right)\right]^{-1}$$
$$[\mathrm{cm}^2\,(V \cdot s)^{-1}] \tag{6}$$

where p represents the hole concentration in cm^{-3} and m_h the hole conductivity-effective mass. The mobility was calculated from $\mu = (\mu_\mathrm{L}^{-1} + \mu_\mathrm{I}^{-1} + \mu_\mathrm{cc}^{-1})^{-1}$.

Two types of fitting analyses were performed: in the dark (0 sun) and under sunlight (1–16 sun). For the first analysis, μ_L and μ_I of Equation (1) and (2) were considered and A and B were used to fit the experimental results in the dark. This is because mobility observed in the dark must be accurately reproduced. Carrier–carrier scattering was not considered because its effect was too small compared to Equation (1) and (2) and had no effect in the dark. The fitting parameters obtained in the dark for A and B were fixed and used for the second fitting analysis under sunlight irradiation (1–16 suns). In particular, the μ_L was temperature dependent but independent of the concentrated illumination. In the second analysis, only the photoexcited electron concentration (Δn) was a fitting parameter. In this study, n in Equation (4) was modified using Δn as $n = \Delta n + N_\mathrm{I}$. N_I is the number of ionized impurity atoms and represents the carrier concentration in the dark. In this study, N_I was $5 \times 10^{15}\,\mathrm{cm}^{-3}$ considering the impurity concentration of the samples. In addition, pn in Equation (6) was modified as $pn = \Delta n(\Delta n + N_\mathrm{I})$ because the photoexcited hole concentration was assumed to

be equal to Δn because a pair of carriers was excited ($p = \Delta p = \Delta n$). Equation (1)–(6) were used to fit the mobility data in Section 3.1, but not those in Section 3.3.

Carriers with higher energies generated by concentrated illumination may have a large effective mass owing to the non-parabolicity of the conduction and valence bands. To consider the effect of the effective mass on mobility due to lattice scattering, we modified Equation (1) as follows:

$$\mu_{\mathrm{Lm}} = A' \times m_{\mathrm{e}}^{-\frac{5}{2}} \times T^{\mathrm{B}} \,[\mathrm{cm}^2(\mathrm{V}\cdot\mathrm{s})^{-1}] \qquad (7)$$

The relationship between the mobility due to lattice scattering and m_{e} is extracted from ref. [23]. Because the literature value of m_{e} in Si is $0.26m_0$, where m_0 represents the mass of a free electron,[23] the A' in Equation (7) was adjusted to be consistent with Equation (1) when the effective mass is $0.26m_0$. Equation (2) and (6) do not need to be modified because they are already functions of the effective mass. Equation (2), (6), and (7) are used in Section 3.2.

2.2.2. Solar Cell Properties

The following numerical calculations for the solar cells were performed using COMSOL Multiphysics to discuss the effect of reduced mobility on the solar cell properties.[24] The solar cell structure was obtained from the application gallery of COMSOL Multiphysics.[24] A pn-junction Si solar cell with a 0.5 mm thick p-type on a 150 mm thick n-type substrate was modeled. The donor and acceptor concentrations were 1.0×10^{16} and 1.0×10^{19} cm^{-3}, respectively. Although mobility varied with impurity concentration, the relationship between impurity concentration and mobility was not considered in the solar cell calculation model because, in this study, we discuss the effect of mobility reduction on solar cell characteristics. Because the geometry of the electrodes was not considered in this study, a 1D model was sufficient. AM1.5G spectra and the absorption coefficients of Si were used.[23,25] Sunlight was illuminated on the 0.5 mm thick p-type side. By solving the Poisson and drift-diffusion equations, the current–voltage characteristics of solar cells can be calculated, allowing the conversion efficiency, fill factor (FF), I_{sc}, V_{oc}, and R_{s} to be calculated. Among the reported methods for calculating R_{s},[26–29] we used the simplest slope method, with the equation $R_{\mathrm{s}} = \frac{dV}{dI}\big|_{I=0}$.[26] This method can uniquely calculate the series resistance without knowing the diode's ideality factor and is considered reasonable for discussing the effect of mobility on the series resistance.

Figure 1 shows the previously reported SC dependence on mobility.[14] The decrease in mobility was used to calculate the solar cell characteristics, as described in Section 3.3. As the observed mobility under concentrated illumination decreased linearly from 1 to 16 suns, we assumed that this linearity remained above 16 suns up to 30 suns. Therefore, the electron and hole mobilities as a function of SC were expressed as $\mu_{\mathrm{e}} = -11 \times \mathrm{SC} + 1175$ and $\mu_{\mathrm{h}} = -3.2 \times \mathrm{SC} + 289\,[\mathrm{cm}^2(\mathrm{V}\cdot\mathrm{s})^{-1}]$, respectively, where SC denotes sunlight concentration. Note that this reduced mobility owing to sunlight illumination is not due to the temperature increase caused by the SC, as mentioned in Section 2.1. The experimentally obtained SC-dependent
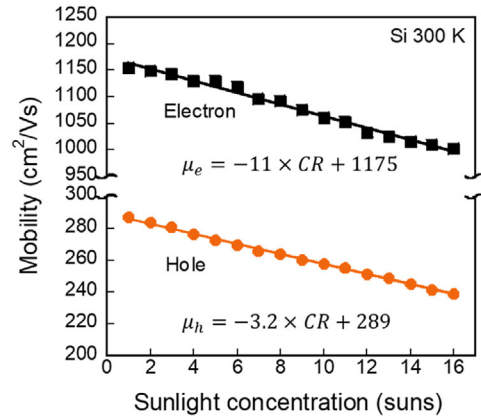

Figure 1. Experimental data of mobilities as a function of SC. The equations in the figure were the fitting results of the mobility from 1 to 16 suns. This figure was reproduced from ref. [14]. The Japanese Journal of Applied Physics does not require permission to reuse figures for which we are the authors.

mobilities were substituted into COMSOL Multiphysics software to calculate the solar cell properties.

3. Results and Discussion

3.1. Carrier Scattering

Figure 2a shows the temperature dependence of the electron mobility under 1, 5, 10, and 16 suns illumination. The symbols represent the experimental data and the curves represent the fitting results. Equation (1), (2), and (6) were used for the fitting. The photoexcited carrier concentration was used as the fitting parameter. This experimental result for the temperature- and SC-dependent carrier mobilities is reported for the first time. The mobility decreases with increasing temperature, as indicated by the dotted arrows. This is mainly due to lattice scattering. The mobility also decreases with increasing SC, as indicated by the direction of the open arrow. As mentioned in Section 1, this decrease was not due to an increase in temperature caused by concentrated illumination or the degradation of the sample. The observed temperature increase with 16 suns illumination under temperature-controlled conditions was 0.045 °C, as measured by a thermocouple near the back of the sample. The calculated temperature rise under 16 suns illumination under temperature-controlled conditions using COMSOL Multiphysics was 0.046 °C, in agreement with the experimental results. The expected decreases in electron and hole mobilities due to the temperature changes were 0.41 and 0.14 cm^2 Vs^{-1}, respectively. The decrease in the experimentally measured electron and hole mobilities from 0 to 16 suns at 300 K was 162.5 and 51.0 cm^2 Vs^{-1}, respectively. Therefore, the temperature increase owing to sunlight illumination was not the reason for the observed decrease in mobility.

First, a fitting analysis of the electron mobility as a function of temperature in the dark was performed using A and B in Equation (1). Consequently, $A = 2.35 \times 10^7$ and $B = -1.73$ were obtained. The fit results are fixed in the following discussion.
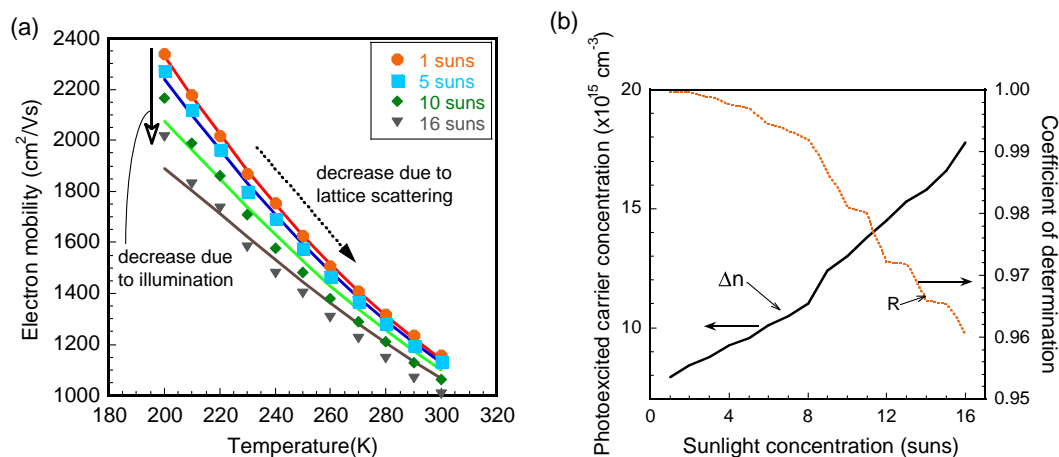
Figure 2. a) Temperature dependence of the mobilities under 1, 5, 10, and 16 suns. The symbols represent the experimental data, and the curves represent the fitting results. Equation (1), (2), and (6) were used for the fitting. The fitting parameter was a photoexcited carrier concentration. b) Fitting results of the photoexcited carrier concentration and the coefficient of determination. The solid and dotted curves were the photoexcited carrier concentration and coefficient of determination (R), respectively.

Second, the fitting analysis under sunlight irradiation was performed using Δn as the fitting parameter in Equation (5) and (6). The experimental and fitting results agreed well for 1 sun but not for 16 suns, as shown in Figure 2a. The experimental results for 16 suns deviated up and down from the calculated curve in the lower and higher temperature regions, respectively. Figure 2b shows the fitting parameter of photoexcited carrier concentration (Δn) and the coefficient of determination as a function of SC. As expected, Δn increased with increasing SC. However, the coefficient of determination decreased by $\approx 4\%$ with an increase in the SC. This reduction indicates that fitting using Equation (1)–(6) cannot explain the decrease in mobility due to the SC. The same result was observed for the holes. In conclusion, the lattice, ionized impurities, and carrier–carrier scattering cannot explain the decrease in mobility due to sunlight illumination. Therefore, other scattering mechanisms should be considered, or the above scattering mechanisms should be modified.

3.2. Effective Masses and Carrier Mobility

The nonparabolicity of the bands increases the effective mass when carriers have higher energies and occupy higher energy of the density of states of the band.[30–33] In our experiment, the AM1.5G spectra were used in the wavelength range of 350–1100 nm (3.54–1.12 eV).[25] Photoexcited carriers have higher energy than the conduction band minimum and can have larger effective masses owing to the nonparabolicity of the bands. Larger effective masses decrease mobility.

To discuss the effect of the electron effective mass m_e on mobility, we considered Equation (2), (6), and (7) for ionized impurities, carrier–carrier, and lattice scattering, respectively, where A' and B in Equation (7) were 8.12×10^5 and -1.73, respectively. This is because A' was adjusted to be consistent with $A = 2.35 \times 10^7$ in Equation (1) when the effective mass was $0.26m_0$, and B was the same between Equation (1) and (7). In other words, Equation (1) and (7) are the same as in the dark.

Figure 3 shows the relationship between the mobility and electron effective mass of each scattering mechanism at 300 K, calculated using Equation (2), (6), and (7). The mobility of each scattering mechanism decreased with increasing m_e. As for ionized impurity and carrier–carrier scattering, photoexcited carrier concentration Δn was set to be 8×10^{14} cm^{-3}, as measured under the photoexcited carrier concentration at 16 suns.[14] However, the changes were small for ionized impurities and carrier–carrier scattering compared to lattice scattering, as shown in Figure 3. Because a larger mobility has little effect on the net mobility, as shown by Matthiessen's rule, we next focused on the effective mass of lattice scattering.

A fitting analysis of the temperature-dependent carrier mobility under SC was performed for the lattice, ionized impurity, and carrier–carrier scattering, where m_e indicates the fitting
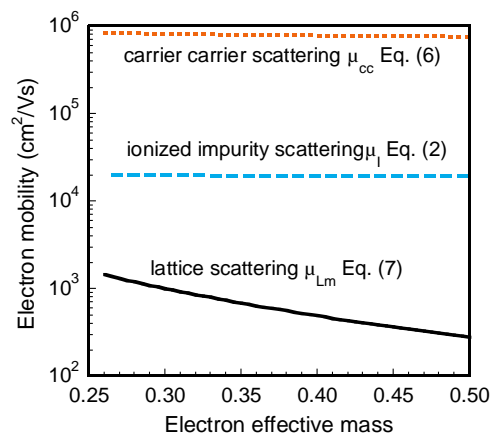

Figure 3. Relationship between electron effective mass (m_e) and calculated electron mobility of each scattering mechanism. Solid, dashed, and dotted curves were mobility due to lattice, ionized impurity, and carrier–carrier scattering. Equation (2), (6), and (7) were used for calculation. The calculated temperature was 300 K.
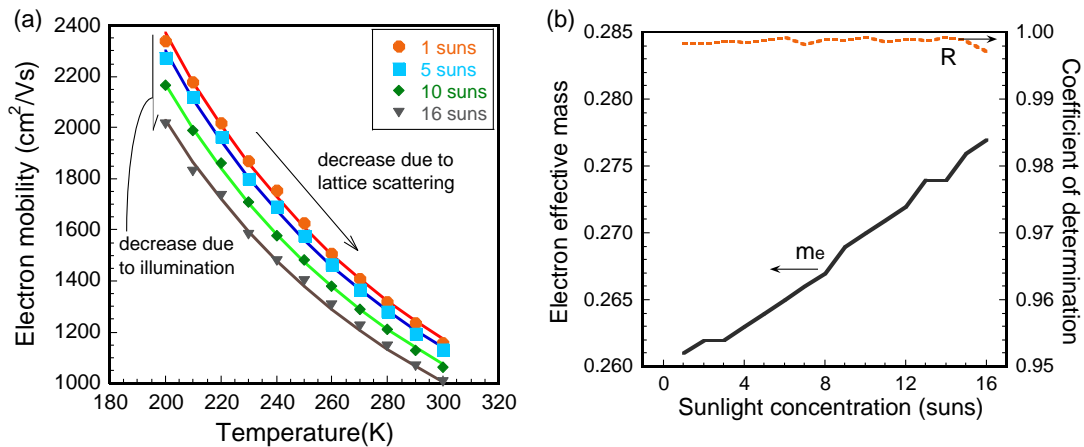
Figure 4. a) Temperature dependence of the mobilities under 1, 5, 10, and 16 suns. The symbols represent the experimental data, and the curves represent the fitting results. Equation (2), (6), and (7) were used for fitting. The fitting parameter was m_e. b) Fitting results of m_e and coefficient of determination. Solid and dashed curves were photoexcited carrier density and coefficient of determination (R), respectively.

parameter, using Equation (2), (6), and (7). The fitting results are shown in **Figure 4**a. The fitting curve agrees well with the experimental results, as shown in Figure 4a, and the coefficient of determination is close to 1 for each SC, as shown in Figure 4b. The discrepancy between the experimental and fitted results, as shown in Figure 2a, was now resolved. In this case, the best-fit m_e increased from $0.26m_0$ to $0.28m_0$ with increasing SC. This increment of $0.02m_0$ is discussed in the following paragraphs.

In the band diagram of Si in momentum space, the conduction band minimum is located on the Δ lines to the X point along the crystallographic [100] direction. This valley is referred to as the Δ valley in this study. The value of m_e at the Δ valley is reported to be $0.26m_0$ when the carrier concentration is small,[23] which is close to the fitting result of $0.26m_0$ at 1 sun. When sunlight irradiates and the number of electrons increases, the higher lying valleys at point L along the [111] direction may also contribute to conduction. The reported electron effective masses in the L valley in the longitudinal and transverse directions are $1.89m_0$ and $0.13m_0$ from ref. [34], or $1.74m_0$ and $0.13m_0$ from ref. [35], respectively. Thus, the mean effective mass in valley L was $0.19m_0$. This value was too small to fit the experimental results. Consequently, the electrons in the L valleys were not responsible for the experimentally observed decrease in mobility.

In the literature, the increase in the effective mass with increasing carrier concentration has been discussed using the nonparabolicity of the band.[30–33] Miyao et al. prepared a highly doped Si substrate and determined the relationship between the carrier concentration and m_e from reflection and absorption spectra.[30] Driel also calculated the relationship between the carrier concentration and effective mass (m_e and m_h) using the pseudopotential method.[31] Their results showed m_e and m_h increased from $0.28m_0$ to $0.50m_0$ and $0.36m_0$ to $1.0m_0$, respectively, when electron and hole concentration increased from 10^{19} to 10^{21} cm^{-3}.[30,31]

The increase in the effective mass owing to the nonparabolicity of this band decreases the mobility under sunlight irradiation. Sunlight irradiation causes electrons to occupy higher energy

states in the conduction band. As mentioned in Section 3.1, the measured photoexcited carrier concentration at 16 suns was 8×10^{14} cm^{-3} in our previous study.[14] Because the effective mass increases at carrier concentrations above 10^{19} cm^{-3}, as reported in refs. [30,31], the photoexcited carrier concentration may be too small to increase the m_e. Only a minimal increase in the effective mass, $\approx 0.02m_0$ could explain the observed results. However, a few photoexcited carriers are insufficient to understand the increase in effective mass. Another possible reason for the mobility decrease is the change in A' in Equation (7). This parameter includes the elastic constant and displacement of the edge of the band per unit dilation of the lattice.[23] The effect of concentrated illumination on them is not clear. Although no conclusive explanation for the change in mobility was obtained, a small change in the coefficient of lattice scattering (A in Equation (1)) could be the reason for the decrease in mobility.

3.3. Solar Cell Properties and Carrier Mobility

In this section, we discuss the effects of sunlight irradiation and decreased mobility on solar cell properties. The solar cell characteristics were calculated by reducing the mobility, as discussed in the previous section. **Table 1** lists the parameters used in these

Table 1. Parameters used in the calculation.[14,23,25]

	Constant mobility case	Decreasing mobility case
Electron mobility [cm^2 Vs^{-1}]	1175	$-11 \times$ SC + 1175
Hole mobility [cm^2 Vs^{-1}]	289	$-3.2 \times$ SC + 289
Carrier lifetime	10 or 1 ms	
Surface recombination [cm s^{-1}]	0	
Solar spectrum	AM1.5G[25]	
Reflectance at the surface [%]	0	
Optical absorption coefficient [cm^{-1}]	18–4.2 × 10^5 (wavelength dependent)[23]	

calculations. The carrier lifetimes were set to 10 and 1 ms to discuss the solar cell properties in more detail, as shown in **Figure 5**. First, we discuss the case of a lifetime of 10 ms. The equation shown in the inset of Figure 1 was used to determine the mobilities of both electrons and holes. Hereafter, we refer to this case as decreasing mobility. The calculated SC dependences of the R_s and the conversion efficiency are shown in Figure 5a. R_s decreased with increasing SC because the number of photoexcited carriers increased and the resistivity of the semiconductor layer decreased. For comparison, the SC-dependent R_s, where the mobility was not changed by irradiation, is also plotted in the figure, referring to the constant mobility case. R_s increased by 4.5 mΩ at 30 suns. Because the mobility decreases with increasing SC, the difference in R_s between the two cases increases at higher SC. The increase in the semiconductor resistance due to decreased mobility is reflected in the increase in R_s.

The conversion efficiency increased with increasing SC, as shown in Figure 5a, because the conversion efficiency of the concentrator solar cells increased with the logarithm of SC. Compared to the case of constant mobility, the conversion efficiency was reduced by 0.19% owing to the decreased mobility at 30 suns. The difference between the two cases (constant or decreasing mobility) increased as the SC increased.

The calculated SC dependences of the V_{oc} are shown in **Figure 6**. The V_{oc} in the decreasing mobility case was higher than that in the constant mobility case. The V_{oc} was expressed by the following equation: $V_{oc} = \frac{k_B T}{q} \ln\left(1 + \frac{I_{sc}}{I_s}\right)$, where I_s denotes the reverse saturation current. Because the I_{sc} was reduced by 27 mA at 30 suns with decreased mobility case (not shown here), the V_{oc} was expected to decrease compared to the constant mobility case. However, this was not observed in this study because of the reduction in I_s. Decreasing the mobility resulted in a lower I_s and higher V_{oc}. If I_{sc} and I_s are proportional to the mobility, V_{oc} will not change. This increase in V_{oc} suggests that I_{sc} and I_s cannot be expressed as simple functions of the mobility, as shown in ref. [10]. FF, which is not shown here, remained constant as a function of SC.

The calculation results when the carrier lifetime is set to 1 ms are shown in Figure 5b. The R_s was increased by 2.4 mΩ at 30 suns because of decreased mobility. The increase in R_s
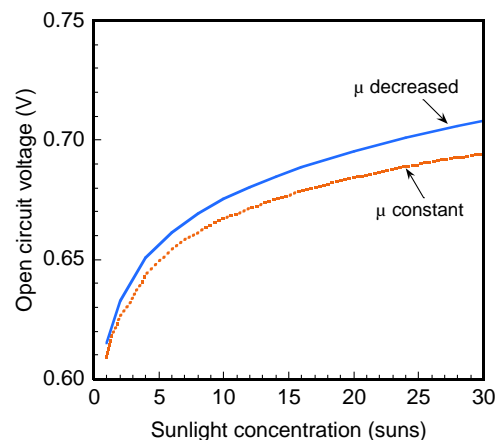

Figure 6. SC dependence of V_{oc} for decreasing (solid curve) and constant mobility (dotted curve) cases. The carrier lifetime was set to 10 ms; however, almost the same results were obtained with 1 ms.

was suppressed compared to the case when the carrier lifetime was 10 ms. The longer carrier lifetime suggests that the increase in R_s was suppressed even when the mobility decreased because of the longer carrier diffusion length. Conversely, contrary to expectations, the conversion efficiency increased by 0.25% in the case of decreasing mobility. This result may be related to the increase in V_{oc} owing to the decrease in mobility described in the previous paragraph; however, the reason behind this is not clear. It was found that for a high SC of 50 suns or more, the conversion efficiency was lower in the case of decreasing mobility because of R_s (not shown here). However, at low concentrations, the conversion efficiency could be higher with smaller mobility. In concentrator solar cells, higher mobility does not necessarily result in better performance, and there may be optimal mobility depending on the carrier lifetime and SC.

As stated before, m_e and m_h increased steeply when the carrier concentration is larger than 10^{20} cm^{-3}.[30,31] Therefore, above a critical SC, there is a steep increase in the effective mass and a decrease in mobility, which can result in a considerable deterioration in solar cell performance. In addition, the increase in R_s
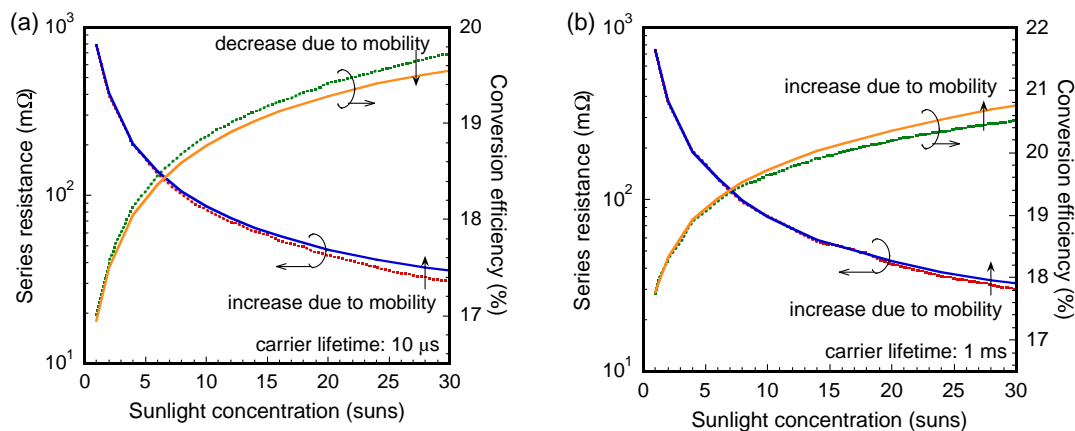

Figure 5. a) SC dependence of R_s and conversion efficiency for decreasing (solid curve) and constant mobility (dotted curve) cases. The difference between a,b) was the carrier lifetime. The carrier lifetime was a) 10 ms and b) 1 ms.

and decrease in conversion efficiency, as shown in Figure 5, did not include a decrease in mobility due to the temperature rise. In actual solar cells, mobility decreases with increasing temperature, which can become dominant and degrade solar cell performance.

4. Conclusion

We have previously reported that concentrated sunlight illumination decreases carrier mobility.[14] However, the reason for this decrease was not apparent. Although we discussed three possible mechanisms such as lattice, ionized impurities, and carrier–carrier scattering, none of them could explain the decrease in carrier mobility. Hence, we considered the increased effective mass as a possible cause of the decreased mobility. The effective masses increased owing to the nonparabolicity of the bands when sunlight irradiation caused electrons to occupy higher energy states in the conduction band. However, the observed low carrier concentration was insufficient to understand the effective mass increase quantitatively. If the effective mass did not increase owing to the concentrated illumination, the coefficient of lattice scattering (A') may have changed. Both are the coefficients of lattice scattering. A slight change in the lattice scattering coefficient was responsible for the decrease in mobility.

The dependence of solar cell performance, such as conversion efficiency and V_{oc}, on concentrated sunlight illumination was theoretically calculated by considering the decrease in mobility as a function of the SC observed in this study. As the mobility decreased, I_{sc} decreased and R_s increased. Meanwhile, the reduced mobility decreased or increased the conversion efficiency depending on the carrier lifetime. When the carrier lifetime was 10 and 1 ms, the conversion efficiencies were decreased by 0.19% but increased by 0.25%, and the R_s increased by 4.5 and 2.4 mW at 30 suns, respectively. Higher mobility does not necessarily result in better performance, and there may be optimal mobility depending on the carrier lifetime and SC. Note that R_s always increases with decreasing mobility. In this study, the mobility decreased due to illumination, and the temperature increase was considered separately. However, both need to be considered simultaneously to discuss solar cell characteristics.

An increase in the effective mass due to band nonparabolicity has also been reported for GaAs.[36] Most semiconductor materials exhibit band nonparabolicity. Therefore, the decrease in mobility due to concentrated sunlight irradiation must be considered for almost all solar cell materials to achieve higher performance if the effective mass is the cause of reduced mobility.

Conflict of Interest

The authors declare no conflict of interest.

Data Availability Statement

The data that support the findings of this study are available from the corresponding author upon reasonable request.

[1] N. Gilmore, V. Timchenko, C. Menictas, *Renewable Sustainable Energy Rev.* **2018**, *90*, 1041.

[2] M. Yamaguchi, T. Takamoto, K. Araki, N. Kojima, *Jpn. J. Appl. Phys.* **2016**, *55*, 04EA05.

[3] C. Domínguez, N. Jost, S. Askins, M. Victoria, I. Antón, *AIP Conf. Proc.* **2017**, *1881*, 080003.

[4] K. Shanks, S. Senthilarasu, T. K. Mallick, *Renewable Sustainable Energy Rev.* **2016**, *60*, 394.

[5] P. Pérez-Higueras, E. Muñoz, G. Almonacid, P. G. Vidal, *Renewable Sustainable Energy Rev.* **2011**, *15*, 1810.

[6] T. Masuda, K. Araki, K. Okumura, S. Urabe, Y. Kudo, K. Kimura, T. Nakado, A. Sato, M. Yamaguchi, *Sol. Energy* **2017**, *146*, 523.

[7] D. Sato, K. H. Lee, K. Araki, T. Masuda, M. Yamaguchi, N. Yamada, *Prog. Photovoltaics Res. Appl.* **2019**, *27*, 501.

[8] M. Yamaguchi, T. Masuda, K. Araki, D. Sato, K. H. Lee, N. Kojima, T. Takamoto, K. Okumura, A. Satou, K. Yamada, T. Nakado, Y. Zushi, M. Yamazaki, H. Yamada, *Energy Power Eng.* **2020**, *12*, 375.

[9] M. Yamaguchi, T. Masuda, K. Araki, D. Sato, K. H. Lee, N. Kojima, T. Takamoto, K. Okumura, A. Satou, K. Yamada, T. Nakado, Y. Zushi, Y. Ohshita, M. Yamazaki, *Prog. Photovoltaics: Res. Appl.* **2021**, *29*, 684.

[10] A. Luque, S. Hegedus, in *Handbook of Photovoltaic Science and Engineering*, John Wiley & Sons Ltd, Chichester, UK **2003**, p. 91.

[11] K. Nishioka, T. Takamoto, T. Agui, M. Kaneiwa, Y. Uraoka, T. Fuyuki, *Sol. Energy Mater. Sol. Cells.* **2006**, *90*, 1308.

[12] T. Takamoto, M. Kaneiwa, M. Imaizumi, M. Yamaguchi, *Prog. Photovoltaics Res. Appl.* **2005**, *13*, 495.

[13] C. Algora, V. Diaz, *Prog. Photovoltaics: Res. Appl.* **2000**, *8*, 211.

[14] T. Harada, N. Miyashita, T. Ikari, A. Fukuyama, *Jpn. J. Appl. Phys.* **2020**, *59*, 71002.

[15] S.-H. Turren-Cruz, M. Saliba, M. T. Mayer, H. Juárez-Santiesteban, X. Mathew, L. Nienhaus, W. Tress, M. P. Erodici, M.-J. Sher, M. G. Bawendi, M. Grätzel, A. Abate, A. Hagfeldt, J.-P. Correa-Baena, *Energy Environ. Sci.* **2018**, *11*, 78.

[16] L. J. Van der Pauw, *Philips Res. Rep.* **1958**, *13*, 1.

[17] C. Kasl, M. J. R. Hoch, *Rev. Sci. Instrum.* **2005**, *76*, 033907.

[18] M. Lundstrom, in *Fundamentals of Carrier Transport*, 2nd ed., Cambridge University Press, Cambridge **2000**, p. 189.

[19] N. D. Arora, J. R. Hauser, D. J. Roulston, *IEEE Trans. Electron Devices* **1982**, *29*, 292.

[20] S. S. Li, W. R. Thurber, *Solid State Electron.* **1977**, *20*, 609.

[21] J. M. Dorkel, P. Leturcq, *Solid State Electron.* **1981**, *24*, 821.

[22] N. H. Fletcher, *Proc. IRE* **1957**, *45*, 862.

[23] S. M. Sze, in *Physics of Semiconductor Devices*, 2nd ed., John Wiley & Sons, New York **1981**, p. 22.

[24] COMSOL AB, COMSOL Multiphysics v, 5.6, Stockholm, Sweden **2020**.

[25] NREL, Reference Air Mass 1.5 Spectra.

[26] S. Daliento, L. Lancellotti, *Sol. Energy* **2010**, *84*, 44.

[27] D. Pysch, A. Mette, S. W. Glunz, *Sol. Energy Mater. Sol. Cells* **2007**, *91*, 1698.

[28] M. Tripathy, M. Kumar, P. K. Sadhu, *Sol. Energy* **2017**, *158*, 432.

[29] K. Tada, *Appl. Phys. Express* **2021**, *14*, 046502.

[30] M. Miyao, T. Motooka, N. Natsuaki, T. Tokuyama, *Solid State Commun.* **1981**, *37*, 605.

[31] H. M. van Direl, *Appl. Phys. Lett.* **1984**, *44*, 617.

[32] M. A. Green, *J. Appl. Phys.* **1990**, *67*, 2944.

[33] D. M. Riffe, *J. Opt. Soc. Am. B* **2002**, *19*, 1092.

[34] F. Murphy-Armando, S. Fahy, *Phys. Rev. B* **2008**, *78*, 035202.

[35] M. M. Rieger, P. Vogl, *Phys. Rev. B.* **1993**, *48*, 14276.

[36] W. G. Spitzer, J. M. Whelan, *Phys. Rev.* **1959**, *114*, 59.